79-4020

Fast, Conservative Schemes for the Full Potential Equation Applied to Transonic Flows

Terry L. Holst* and William F. Ballhaus†
NASA Ames Research Center, Moffett Field, Calif.

Implicit approximate factorization techniques (AF) are investigated for the solution of matrix equations resulting from finite-difference approximations to the full potential equation in conservation form. For transonic flows, an artificial viscosity, required to maintain stability in supersonic regions, is introduced by an upwind bias of the density. Two implicit AF procedures are presented, and their convergence performance is compared with that of the standard transonic solution procedure: successive line overrelaxation (SLOR). Subcritical and supercritical test cases are considered. Results indicate a substantial improvement in convergence rate for AF schemes relative to SLOR.

I. Introduction

THERE are basically three formulations for inviscid transonic flows. These are, in order of increasing complexity (and in order of decreasing approximation), 1) transonic small-disturbance potential equation (TSD), 2) full potential equation (FP), and 3) Euler equations (exact inviscid formulation). TSD is valid for thin wings at freestream Mach numbers near unity and is an isentropic and irrotational formulation. It offers the advantage of simplicity, especially in the treatment of wing surface boundary conditions. The FP formulation can be considered exact under the assumptions of irrotational and isentropic flow. These assumptions, which are less restrictive than those for TSD, are valid for a wide range of practical transonic flows. Potential formulations can be written in terms of a single second-order partial differential equation (PDE), whereas the Euler formulation consists of a set of first-order PDE's (usually four in two-dimensional cases). Hence, for implicit AF schemes the potential formulations require only scalar matrix operations, whereas the Euler formulation requires time-consuming block matrix operations. The FP formulation is the most efficient of the three formulations in terms of accuracy-to-cost ratio for a wide range of inviscid transonic flow applications.

The object of this investigation has been to determine the feasibility of using implicit approximate factorization algorithms (AF) to solve the full potential equation in conservation form for steady transonic flowfields. The two AF schemes tested are logical extensions of the schemes previously developed for the TSD equation.[1,2] These previous studies found the AF approach to be substantially faster than the standard transonic flowfield solution procedure, successive line overrelxation (SLOR).

Section II begins with a discussion of the full potential equation in conservation form. Spatial difference approximations then are introduced, including the addition of artificial viscosity required to maintain stability in supersonic zones. The difference approximations are equivalent to those introduced by Jameson.[3] Here, however, the artifical viscosity is not introduced explicitly, as in the Jameson approach, but rather by retarding the density.

In Sec. III, two implicit AF iteration schemes are presented. AF and SLOR convergence histories than are compared in Sec. IV for both subcritical and supercritical cases. Results indicate a substantial increase in computational efficiency for the AF schemes over an SLOR scheme.

Received March 28, 1978; revision received Aug. 11, 1978. This paper is declared a work of the U.S. Government and therefore is in the public domain.

Index categories: Transonic Flow; Computational Methods.

*Research Scientist. Member AIAA.

†Research Scientist, Aeromechanics Laboratory, U.S. Army Research and Technology Laboratories (AVRADCOM). Associate Fellow AIAA.

II. Spatial Differencing of the Full Potential Equations in Conservation Form

A. Full Potential Equation

The full potential equation written in conservation-law form is given by

$$(\rho\phi_x)_x + (\rho\phi_y)_y = 0 \tag{1}$$

where

$$\rho = \left[1 - \frac{\gamma-1}{\gamma+1}\left(\phi_x{}^2 + \phi_y{}^2\right)\right]^{1/\gamma-1} \tag{2}$$

In Eqs. (1) and (2), the density ρ and velocity components ϕ_x and ϕ_y are nondimensionalized by the stagnation density ρ_s and the critical sound speed a^*, respectively; x and y are Cartesian coordinates, and γ is the ratio of specific heats.

Equations (1) and (2) express mass conservation for flows that are isentropic and irrotational. The corresponding shock-jump conditions are valid approximations to the Rankine-Hugoniot relations for many transonic flow applications. A comparison of the isentropic and Rankine-Hugoniot shock polars is given in Ref. 4.

It is essential that the finite-difference approximation to Eq. (1) be cast in conservation form.[5] Otherwise, the shock-capturing procedure will not necessarily conserve mass across the shock wave.[3] Nonconservative rather than conservative difference schemes have been used in many engineering applications. However, the nonconservative procedures introduce mass sources at shock waves, and the strength of these sources depends on the local grid spacing, a nonphysical consideration. Erroneous shock solutions therefore result.

B. Spatial Differencing in One Dimension

To begin with, consider the one-dimensional version of Eq. (1):

$$(\rho\phi_x)_x = 0 \tag{3}$$

A second-order accurate finite-difference approximation to Eq. (3) is given by

$$\delta_x \rho_{i+(1/2)} \delta_x \phi_i = 0 \tag{4}$$

where $\overleftarrow{\delta}_x$ and $\overrightarrow{\delta}_x$ are backward and forward difference operators defined by

$$\overleftarrow{\delta}_x \phi_i = \Delta x^{-1}(\phi_i - \phi_{i-1}) \tag{5a}$$

$$\overrightarrow{\delta}_x \phi_i = \Delta x^{-1}(\phi_{i+1} - \phi_i) \tag{5b}$$

Equation (4) is a suitable finite-difference scheme for subsonic flow regions; however, for supersonic regions, a properly chosen artificial viscosity term must be added. For example, Jameson[3] adds the following viscosity term:

$$-\Delta x(\mu \phi_{xx})_x \tag{6}$$

where $\mu = \min[0, \rho(1 - \phi_x{}^2/a^2)]$. This is analogous to the switching used in the Murman mixed-difference procedure.[6] It can be shown[3] [by differentiating the one-dimensional form of Eq. (2)] that this is equivalent to adding

$$-\Delta x(\nu \rho_x \phi_x)_x \tag{7}$$

where $\nu = \max[0, (1 - a^2/\phi_x{}^2)]$. The complete finite-difference approximation to Eq. (3) thus can be written as

$$(\rho\phi_x)_x \approx \overleftarrow{\delta}_x \rho_{i+(\frac{1}{2})} \overrightarrow{\delta}_x \phi_i - \overleftarrow{\delta}_x \nu_i [\rho_{i+(\frac{1}{2})} - \rho_{i-(\frac{1}{2})}] \overrightarrow{\delta}_x \phi_i = 0 \tag{8}$$

[Other difference approximations to Eq. (7) are possible, and some of these will be discussed in a subsequent section.] This scheme is centrally differenced and second-order accurate in subsonic regions. In supersonic regions, the differencing is a combination of the second-order-accurate central differencing used in subsonic regions and the first-order-accurate upwind differencing resulting from the addition of artificial viscosity. As the flow becomes increasingly supersonic, the scheme is increasingly retarded in the upwind direction.

Equation (8) can be rearranged to give

$$(\rho\phi_x)_x \approx \overleftarrow{\delta}_x \tilde{\rho}_{i+(\frac{1}{2})} \overrightarrow{\delta}_x \phi_i = 0 \tag{9a}$$

where

$$\tilde{\rho}_{i+(\frac{1}{2})} = (1 - \nu_i)\rho_{i+(\frac{1}{2})} + \nu_i \rho_{i-(\frac{1}{2})} \tag{9b}$$

The addition of the artificial viscosity given by Eq. (7) is thus equivalent to retarding the density in Eq. (4). Artificial viscosity is not added explicitly as in the Jameson procedure.[3] However, the two approaches produce identical results. The significance of the present approach will become apparent in the discussion of solution algorithms (Sec. III).

The choice of ν strongly affects the accuracy and stability of solutions to Eq. (9). The particular choice $\nu = \max[0, (1 - a^2/\phi_x{}^2)]$ results in an effective artificial viscosity that corresponds exactly to the form used by Jameson,[3] and generally satisfactory results are obtained. For $\nu = 0$, the difference scheme reduces to Eq. (4), which is unstable for supersonic regions. The choice $\nu = 1$ results in a first-order-accurate approximation that is highly dissipative. However, stable solutions can be obtained for both subsonic and supersonic regions. Computed results for various choices of ν are presented in the following section.

C. Computed Results for the One-Dimensional Case

The effect of ν on shock wave resolution is studied here using a one-dimensional test problem. Computed results for three different shock strengths are shown in Fig. 1. Exact (discontinuous) solutions are indicated by the dashed line. The discrete data are solutions to Eq. (9) for three different choices of ν, representing three different strategies for choosing a value of artificial viscosity by retarding the density. The result, equivalent to the Jameson viscosity which is switched on (in the Murman fashion) only for supersonic

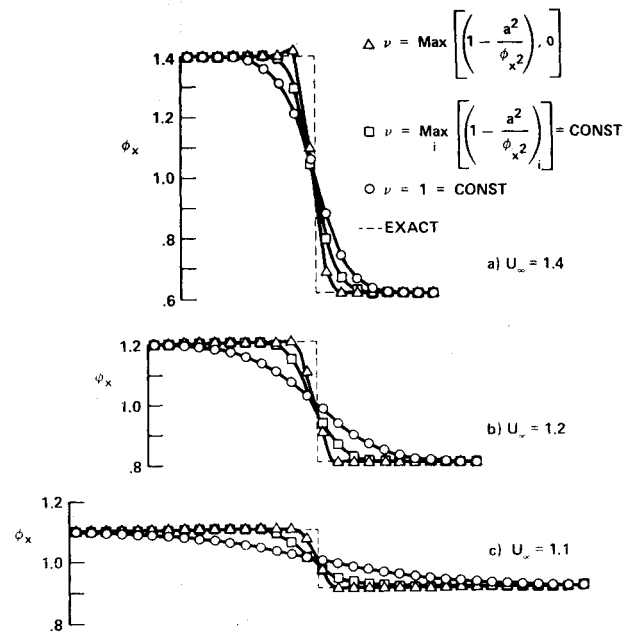

Fig. 1 Shock profiles, ϕ_x vs x.

points, is shown by the triangles. There is a slight overshoot that increases in amplitude with increasing shock strength. Note that the shock is always captured in a distance of about three mesh cell widths.

The two other solutions were computed with ν constant. The density is retarded by the same amount in both subsonic and supersonic regions, so that there is no Murman-type switching. The solutions represented by the squares were computed using a constant value of ν equivalent to that used in the (uniform) supersonic region by the Jameson strategy. Shock waves for this approach are captured in about five to seven mesh cell widths. For the choice $\nu = 1$, shocks are smeared over a substantially greater distance, especially for the weaker shocks.

The results shown in Fig. 1 indicate that the Jameson choice of artificial viscosity, implemented here by retarding the density, is a suitable one for shocks of weak to moderate strength. Furthermore, if one is willing to sacrifice second-order accuracy in subsonic regions and accept a greater degree of shock smearing, solutions can be obtained without switching differences; the test for supersonic flow can thereby be eliminated.

D. Spatial Differences in Two Dimensions

A second-order-accurate finite-difference approximation to Eq. (1) is given by

$$[\overleftarrow{\delta}_x \rho_{i+(\frac{1}{2}),j} \overrightarrow{\delta}_x + \overleftarrow{\delta}_y \rho_{i,j+(\frac{1}{2})} \overrightarrow{\delta}_y] \phi_{i,j} = 0 \tag{10}$$

where $\overleftarrow{\delta}_y$ and $\overrightarrow{\delta}_y$ are backward and forward y-direction difference operators, respectively, defined similarly to the x-direction operators given by Eq. (5). As in the one-dimensional case, Eq. (10) is a suitable finite-difference scheme for subsonic flow regions but not for supersonic flow regions. A properly chosen artificial viscosity term must be added. In two dimensions, Jameson[3] adds an artificial viscosity term of the following form ($v_{i,j+(\frac{1}{2})} > 0$):

$$-\overleftarrow{\delta}_x \nu_{i,j} u_{i+(\frac{1}{2}),j} (\rho_{i+(\frac{1}{2}),j} - \rho_{i-(\frac{1}{2}),j}) - \overleftarrow{\delta}_y \nu_{i,j} v_{i,j+(\frac{1}{2})} (\rho_{i,j+(\frac{1}{2})} - \rho_{i,j-(\frac{1}{2})}) \tag{11a}$$

where $\nu = \max[0, (1 - a^2/q^2)]$. For the case when $v_{i,j+(\frac{1}{2})} < 0$ the artificial viscosity term is slightly different and is given by

$$-\delta_x^{\leftarrow} \nu_{i,j} u_{i+(\frac{1}{2}),j} (\rho_{i+(\frac{1}{2}),j} - \rho_{i-(\frac{1}{2}),j})$$
$$-\delta_y^{\leftarrow} \nu_{i,j+1} v_{i,j+(\frac{1}{2})} (\rho_{i,j+(3/2)} - \rho_{i,j+(\frac{1}{2})}) \quad (11b)$$

For convenience of presentation, only the first case will be considered hereafter. The complete finite-difference approximation to Eq. (1) thus can be written as

$$(\rho\phi_x)_x + (\rho\phi_y)_y \approx [\delta_x^{\leftarrow} \rho_{i+(\frac{1}{2}),j} \delta_x^{\rightarrow} + \delta_y^{\leftarrow} \rho_{i,j+(\frac{1}{2})} \delta_y^{\rightarrow}] \phi_{i,j}$$
$$-\delta_x^{\leftarrow} \nu_{i,j} u_{i+(\frac{1}{2}),j} (\rho_{i+(\frac{1}{2}),j} - \rho_{i-(\frac{1}{2}),j})$$
$$-\delta_y^{\leftarrow} \nu_{i,j} v_{i,j+(\frac{1}{2})} (\rho_{i,j+(\frac{1}{2})} - \rho_{i,j-(\frac{1}{2})}) = 0 \quad (12)$$

This scheme is centrally differenced and second-order accurate in subsonic regions. In supersonic regions, the differencing is a combination of the second-order-accurate central differencing used in subsonic regions and the first-order-accurate upwind differencing resulting from the addition of artificial viscosity. As the flow becomes increasingly supersonic, the scheme is retarded increasingly in the upwind direction.

As in the one-dimensional case, the two-dimensional scheme can be rearranged to give

$$(\rho\phi_x)_x + (\rho\phi_y)_y \approx [\delta_x^{\leftarrow} \tilde{\rho}_{i+(\frac{1}{2})} \delta_x^{\rightarrow} + \delta_y^{\leftarrow} \tilde{\rho}_{j+(\frac{1}{2})} \delta_y^{\rightarrow}] \phi_{i,j} = 0 \quad (13a)$$

$$\tilde{\rho}_{i+(\frac{1}{2})} = (1 - \nu_{i,j}) \rho_{i+(\frac{1}{2}),j} + \nu_{i,j} \rho_{i-(\frac{1}{2}),j} \quad (13b)$$

$$\tilde{\rho}_{j+(\frac{1}{2})} = (1 - \nu_{i,j}) \rho_{i,j+(\frac{1}{2})} + \nu_{i,j} \rho_{i,j-(\frac{1}{2})} \quad (13c)$$

The addition of the artificial viscosity given by Eq. (11) is thus equivalent to retarding the density in Eq. (10). Artificial viscosity is not added explicitly as in the Jameson procedure. However, the two approaches produce identical results. As pointed out by Jameson,[3] the difference scheme given by Eq. (12) provides automatic upwind differencing of the streamwise terms in supersonic regions. Thus the full effect of rotated differencing is included in the present finite-difference scheme.

The present scheme can be extended easily to include an arbitrary coordinate system. For example, transformation of the full potential equation from Cartesian coordinates (x,y) given by Eq. (1) to a general coordinate system (ξ,η) yields the full potential equation in the following form:

$$(\rho U/J)_\xi + (\rho V/J)_\eta = 0 \quad (14)$$

where J is the Jacobian of the transformation, and U and V are the contravariant velocity components along the ξ and η directions, respectively, and are linear functions of ϕ_ξ and ϕ_η. No restrictions have been placed on the (ξ,η) coordinate system, and, for example, nonorthogonal coordinates can be used. This allows considerable flexibility in treating a wide range of geometries.

The spatial differencing scheme for a general (ξ,η) coordinate system can be written as follows:

$$(\rho U/J)_\xi + (\rho V/J)_\eta \approx \delta_\xi^{\leftarrow} \tilde{\rho}_{i+(\frac{1}{2})} (U/J)_{i+(\frac{1}{2}),j}$$
$$+\delta_\eta^{\leftarrow} \tilde{\rho}_{j+(\frac{1}{2})} (V/J)_{i,j+(\frac{1}{2})} = 0 \quad (15)$$

where $\tilde{\rho}_{i+(\frac{1}{2})}$ and $\tilde{\rho}_{j+(\frac{1}{2})}$ are upwind evaluations of the density defined similarly to Eq. (13). The general spatial difference scheme given by Eq. (15) contains all of the properties of the simpler Cartesian version [Eq. (13)]. Namely, this scheme is second-order accurate and centrally differenced in subsonic flow regions. The artificial viscosity is obtained solely by an upwind bias of the density coefficient in both the ξ and η directions. This form of spatial differencing fits nicely into the framework of many iteration procedures. Three procedures will be presented in subsequent sections of this paper. For the sake of simplicity, only the Cartesian form of the full potential equation will be investigated.

III. Implicit Approximate Factorizations

A. General Requirements

A general form for a two-level solution procedure is given by

$$NC^n + \omega R^n = 0 \quad (16)$$

where C^n $(=\phi^{n+1} - \phi^n)$ is the correction, R^n $(=L\phi^n)$ is the residual [defined by Eq. (13a)], which is a measure of how well the finite-difference equation is satisfied by the nth level solution (ϕ^n), and ω is a relaxation parameter. The iteration scheme given by Eq. (16) can be regarded as an iteration in pseudotime, where the n superscript indicates the time-step level of the solution. The operator N determines the type of iterative procedure and, therefore, determines the rate at which the solution procedure converges. In the approximate factorization approach, N is chosen as a product of two or more factors indicated by

$$N = N_1 N_2 \sim L \quad (17)$$

The factors N_1 and N_2 are chosen so that 1) their product is an approximation to L, 2) only simple matrix operations are required, and 3) the overall scheme is stable.

In what follows, three iteration procedures are discussed, each corresponding to a different choice for N. These methods, which involve only simple bidiagonal or tridiagonal matrix operations, are 1) successive line overrelaxation (SLOR), the standard transonic flow solution procedure; 2) alternating direction implicit (ADI), one type of implicit approximate factorization scheme (called AF1 in Ref. 1); and 3) AF2, another type of implicit approximation factorization scheme.

B. Successive Line Overrelaxation (SLOR)

The SLOR algorithm used in the present study can be expressed by choosing N as follows:

$$NC^n_{i,j} = \left[\Delta x^{-1} \left(-\frac{\tilde{\rho}^n_{i+(\frac{1}{2})}}{\Delta x} - \tilde{\rho}^n_{i-(\frac{1}{2})} \delta_x^{\rightarrow}\right) + \delta_y^{\leftarrow} \tilde{\rho}^n_{j+(\frac{1}{2})} \delta_y^{\rightarrow}\right] C^n_{i,j} \quad (18)$$

This difference expression has been time-linearized by evaluating ρ at iteration level n. Because the cross terms are included indirectly in ρ, the form of N chosen here is simpler than the commonly used quasilinear form of the full potential equation. This scheme is implicit in the y direction; that is, the complete y-direction operator is included in N. This requires the inversion of a tridiagonal matrix equation for each x = const line. The operator is explicit in the x direction because it contains only the lower diagonal part of the x-direction operator. This means that each grid point is influenced by only a single grid point to the right in the x direction during one iteration, which contributes to a relatively slow evolution of the solution. Construction of N in a fully implicit manner, however, means that each grid point is influenced by every other grid point during each iteration. As a result, much faster convergence can be obtained. The next two algorithms presented are both fully implicit and obtain this form by constructing N as approximate factorizations of L.

C. Approximate Factorization: Scheme 1 (AF1)

The first fully implicit algorithm is similar to the AF1 scheme presented in Ref. 1, which was used to solve the TSD equation. This scheme, which is a reformulation of the Peaceman-Rachford alternating direction implicit technique (ADI), can be expressed by choosing N as follows:

$$\alpha N C^n_{i,j} = -(\alpha - \delta_x^{\leftarrow} \tilde{\rho}^n_{i+(\frac{1}{2})} \delta_x^{\rightarrow})(\alpha - \delta_y^{\leftarrow} \tilde{\rho}^n_{j+(\frac{1}{2})} \delta_y^{\rightarrow}) C^n_{i,j} \quad (19)$$

where α is a free parameter to be defined subsequently. Note that both the x and y directions are treated implicitly and that N has been written as the product of two factors which, when multiplied out, yield the time-linearized L operator plus two error terms. The first error term is a ϕ_t-type term and, therefore, provides a stabilizing effect to the iteration process in subsonic flow regions but a destabilizing effect in supersonic flow regions.[7] The effect of this term is apparent in the computed results, Sec. IV.

The scheme can be restated in practical terms using two steps as follows:

Step 1

$$[\alpha - \bar{\delta}_x \tilde{\rho}^n_{i+1/2} \vec{\delta}_x] f^n_{i,j} = \alpha\omega L\phi^n_{i,j} \tag{20a}$$

Step 2

$$[\alpha - \bar{\delta}_y \tilde{\rho}^n_{j+(1/2)} \vec{\delta}_y] C^n_{i,j} = f^n_{i,j} \tag{20b}$$

where $f^n_{i,j}$ is an intermediate result stored at each mesh point in the finite-difference mesh. In step 1, the f array is obtained by solving a tridiagonal matrix equation for each y = const line. The correction array ($C^n_{i,j}$) then is obtained in the second step from the f array by solving a tridiagonal matrix equation for each x = const line. Thus, by writing N as the product of two factors, it is possible to obtain a fully implicit technique involving only simple tridiagonal matrix operations.

D. Approximate Factorization: Scheme 2 (AF2)

The second fully implicit algorithm presented here is similar to the AF2 scheme presented in Ref. 1, which was applied to the TSD equation. The AF2 scheme, first investigated by Ballhaus and Steger,[8] can be expressed by choosing N as follows:

$$\alpha N C^n_{i,j} = -(\alpha\bar{\delta}_x - \bar{\delta}_y \tilde{\rho}^n_{j+(1/2)} \vec{\delta}_y)(\alpha - \tilde{\rho}^n_{i+(1/2)} \vec{\delta}_x) C^n_{i,j} \tag{21}$$

where again N has been written as the product of two factors which, when multiplied out, yield the time-linearized L operator plus two error terms. The first error term is an upwind ϕ_{xt}-type term and, therefore, provides time-dependent dissipation for the convergence process, which is especially convenient for supersonic flow. When constructing N in this form, care must be taken to insure that this term has the proper sign and is differenced in the upwind direction, Implementation of the AF2 scheme is achieved by writing it in a two-step form given by the following:

Step 1

$$(\alpha\bar{\delta}_x - \bar{\delta}_y \tilde{\rho}^n_{j+(1/2)} \vec{\delta}_y) f^n_{i,j} = \alpha\omega L\phi^n_{i,j} \tag{22a}$$

Step 2

$$(\alpha - \tilde{\rho}^n_{i+(1/2)} \vec{\delta}_x) C^n_{i,j} = f^n_{i,j} \tag{22b}$$

where $f^n_{i,j}$ is an intermediate result stored at each mesh point in the finite-difference mesh. In step 1, the f array is obtained by solving a tridiagonal matrix equation for each x = const line. The correction array ($C^n_{i,j}$) then is obtained in the second step from the f array by solving a simple bidiagonal matrix equation for each y = const line. Note that with AF2 the x-direction difference approximation is split between two steps. This generates the desired ϕ_{xt} term as mentioned previously and also places a sweep direction restriction on both steps, namely, downwind for the first step and upwind for the second step.

Normally, flowfield, type-dependent differencing is used to achieve stability in transonic flow calculations. Incorporating these different operators into iteration procedures, such as the AF schemes presented here, would be cumbersome if not impossible. Using the upwind bias of the density coefficient, which is always evaluated at the nth iteration level, allows the simple two- and three-banded matrix form of the AF schemes to be retained over the entire flowfield, even in regions of supersonic flow. In fact, use of upwinded density coefficients in any general iteration scheme (i.e., for any arbitrary N operator) could be used to remove the difficulties introduced by type-dependent differencing. The resulting general scheme would retain the same basic differencing (at the $n+1$ iteration level) throughout the entire flowfield, relying on the upwind bias of the density (at the nth iteration level) to provide the artificial viscosity in supersonic flow regions. This represents a significant simplification in the handling of supersonic flow regions for transonic flow calculations.

An apparent difficulty exists in extendiig the present AF2 algorithm to include exact airfoil geometry. This extension requires an arbitrary coordinate mapping ($x,y \rightarrow \xi,\eta$; see Sec. II.D) to transform the airfoil surface into a constant coordinate line of the computational domain. The ξ-coordinate direction controls the direction of the $\phi_{\xi t}$ difference (either upwind or downwind), which means that, on either the upper or lower surface of the airfoil, the $\phi_{\xi t}$ term will be differenced improperly in the downwind direction. A simple way to resolve this difficulty is to split the η derivative in the AF2 factorization instead of the ξ derivative. This generates a $\phi_{\eta t}$-type term in place of the $\phi_{\xi t}$ term. The $\phi_{\xi t}$ term then can be added explicitly in the appropriate factor with a flow direction test to insure upwind differencing. This approach has been used in extending to the exact geometry case and appears to be successful. Details are given in Ref. 9.

E. Selection of α for the Aproximate Factorization Schemes

In both the AF1 and AF2 schemes, the quantity α is an as yet undefined free parameter. If α were chosen to be Δt^{-1}, then both schemes could be considered to be iterations in pseudotime. This provides one strategy for obtaining fast convergence, namely, advance time as fast as possible with large time steps (i.e., small α's). As pointed out in Ref. 1, this is effective for attacking the low-frequency errors but not the high-frequency errors. A better approach is to use an α sequence containing several values of α. The small values are particularly effective for reducing the low-frequency errors, and the large values are particularly effective for reducing the high-frequency errors. End points for a suitable α sequence can be approximated analytically[1]; for the present case, these approximations are given by the following:

AF1

$$\alpha_H = 4\rho/\Delta y^2, \quad \alpha_L = \rho \tag{23}$$

AF2

$$\alpha_H = 1/\Delta y, \quad \alpha_L = 1 \tag{24}$$

where ρ is a representative value of density (e.g., ρ_∞) and Δy is the minimum y-direction spacing in the finite-difference mesh. Refinement of these estimates by numerical experiment increases the efficiency of the iteration procedure. The α sequence used in the present study is given by

$$\alpha_k = \alpha_H (\alpha_L/\alpha_H)^{(k-1)/(M-1)}; \; k = 1,2, \ldots, M \tag{25}$$

where M is the number of elements in the sequence. This (geometric) sequence has been found to be effective,[1] although other sequences perhaps could provide equivalent or improved convergence performance.

IV. Two-Dimensional Results

The three schemes presented in the previous section (SLOR, AF1, and AF2) are evaluated in this section. A two-

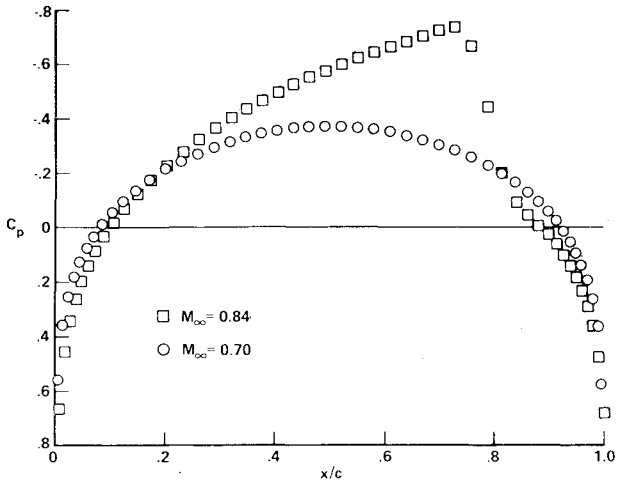

Fig. 2 10% circular arc pressure coefficient distributions.

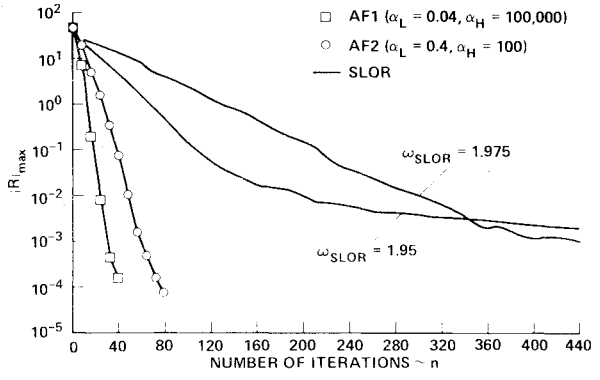

Fig. 3 Maximum residual convergence history comparison (case A).

dimensional, 10% thick circular-arc airfoil with small-disturbance boundary conditions is used as a test case. Both subcritical (case A) and supercritical (case B) Mach numbers are considered. The finite-difference grid is Cartesian, with variable spacing in both the x and y directions. Use of the Cartesian grid with small-disturbance boundary conditions was chosen from the standpoint of simplicity and does not reflect the desired ultimate use of the full potential schemes under investigation.

The subcritical and supercritical pressure coefficient distributions (cases A and B, respectively) are presented in Fig. 2. These results were computed with a 90 × 21 mesh containing 47 points on the airfoil surface. The boundaries were located five chord-lengths away from the airfoil in the x direction and six chord-lengths away in the y direction. In the AF cases, the α sequence contained eight elements ($M = 8$).

A. Convergence Performance for the Subcritical Case

Convergence characteristics for the subcritical case in terms of maximum residual histories are displayed in Fig. 3. The AF results were established by plotting the maximum residual every eighth iteration, which always corresponded to $\alpha = \alpha_L$ in the eight-element sequence. The SLOR results were established by plotting the residual every 20 iterations. All of the convergence parameters (ω_{SLOR}, α_H, and α_L) have been selected by a trial-and-error optimization process. [Results for two choices of relaxation parameter ($\omega_{SLOR} = 1.95$ and 1.975) are presented for SLOR. The larger value produced faster convergence for a maximum residual drop greater than four orders of magnitude, while the smaller value produced faster convergence for smaller drops in the residual.] The relaxation factor used in both the AF1 and AF2 schemes [ω in Eqs. (20) and (22)] was held fixed at 2 for all test cases. Based on a six-order-of-magnitude drop in maximum residual, the AF1 scheme is about twice as fast as the AF2 scheme and about 16 times faster than the SLOR scheme. These speed ratios are in terms of iteration count. The AF1 and AF2 schemes take about 50% and 30% more CPU time per iteration than SLOR. This should be taken into account when considering the speed ratios based on the total amount of computational work.

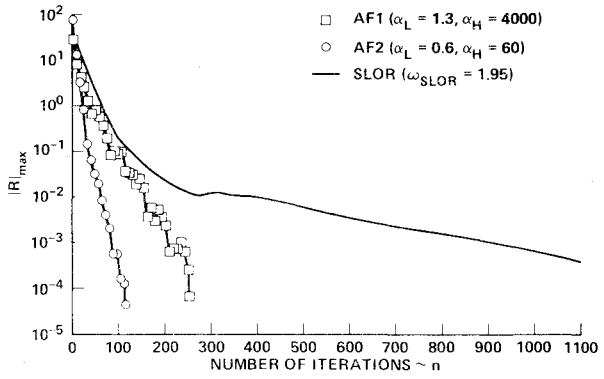

Fig. 4 Maximum residual convergence history comparison (case B).

For several reasons, exact determination of speed ratios for these schemes is difficult to assess. First, use of grid sequences usually provides as much as a factor of 2 speed increase for SLOR schemes but only a small speed increase for the AF schemes.[1] Grid sequences were not used for any results reported here. Second, use of nonoptimal convergence parameters does slow convergence by as much as a factor of 2 or more for both the SLOR and AF schemes. Because the AF schemes have two parameters to optimize (α_H and α_L), as opposed to only one for SLOR (ω_{SLOR}), optimization is more difficult for the AF schemes. Finally, and most important, the AF schemes reduce the errors associated with all frequencies equally well, approximately, whereas the SLOR scheme is efficient for only the high frequencies. Since the residual is heavily biased toward the high-frequency end of the error spectrum, using a specified drop in the maximum residual to define convergence heavily favors the SLOR scheme.[2] More discussion on this last point is provided in Sec. IV.C.

B. Convergence Performance for the Supercritical Case

Convergence characteristics for the supercritical case (case B) in the form of maximum residual histories are displayed in Fig. 4. Again the ω_{SLOR}, α_H, and α_L values have been obtained by trial-and-error optimization. Based on a six-order-of-magnitude drop in the maximum residual and in terms of iteration count, AF2 is slightly more than twice as fast as AF1 and about 11 times faster than SLOR.

The number of supersonic points (NSP) plotted vs iteration number for case B is shown in Fig. 5; the final NSP is 187. The AF2, AF1, and SLOR results reach this level in 29, 103, and 320 iterations, respectively. The small number of iterations required by AF2 to establish the supersonic zone is another indication of how rapidly the solution evolves with this approach.

The AF2 scheme was relatively consistent in convergence speed for both the subsonic and supersonic cases (79 and 118 iterations, respectively). The AF1 scheme, on the other hand, displayed remarkable speed for the subsonic case (39 iterations) but was a disappointment in the supersonic case (254 iterations). Perhaps this is because the ϕ_{xt} error term produced by the AF2 factorization is more suitable for supersonic regions than the ϕ_t error term resulting from the AF1 factorization.

It should be pointed out that use of the standard definition for ν in two dimensions [see Eq. (7)] produced preshock overshoots that often resulted in numerical instability. This instability was experienced for both the standard rotated [see Eq. (13)] and nonrotated difference schemes. [The nonrotated difference scheme simply has no y-direction artificial viscosity

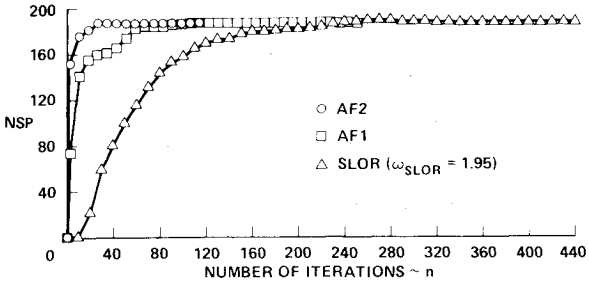

Fig. 5 Development of the supersonic region (case B).

term. This causes the term $(\rho\phi_y)_y$ to remain centrally differenced in supersonic regions.] Therefore, an alternative definition for ν was introduced:

$$\nu = \begin{bmatrix} 1-(\rho/\rho_*)^{\sigma_e} & M>1 \\ 0 & M<1 \end{bmatrix} \tag{26}$$

where ρ_* is the sonic value of density, and σ_e has been chosen by numerical experiment to be six. Use of Eq. (26) instead of the standard definition for ν increases the amount of upwinding or, equivalently, the amount of artificial viscosity in supersonic flow regions. Shock wave overshoots thereby were prevented for the supercritical case presented here.

Several variations of the artificial viscosity term have been investigated. In all cases, only the x-direction artificial viscosity term has been included (i.e., nonrotated differencing). Two of these variations are given by

$$-\delta_x \nu_{i,j} u_{i,j} (\rho_{i+(\frac{1}{2}),j} - \rho_{i-(\frac{1}{2}),j}) \tag{27}$$

$$-\delta_x \nu_{i+(\frac{1}{2}),j} u_{i+(\frac{1}{2}),j} (\rho_{i+(\frac{1}{2}),j} - \rho_{i-(\frac{1}{2}),j}) \tag{28}$$

The artificial viscosity term introduced previously [Eq. (11)] corresponds exactly to the term reported by Jameson.[3] This form is reported incorrectly in that Jameson actually uses the artificial viscosity given by Eq. (27).[10] The artificial viscosity term given by Eq. (28) is still another successful version. All three variations of artificial viscosity (with suitably tailored forms for ν) have been tested for case B and give essentially the same results.

Limited testing of the AF2 algorithm introduced herein at higher freestream Mach numbers (as high as $M\infty = 0.98$) has been conducted. Larger values of α_L and α_H (or equivalently larger amounts of ϕ_{xl}) were required to maintain stability and, therefore, slowed the rate of convergence. It is interesting to note that, for the $M_\infty = 0.98$ case, which has a "fishtail" shock system at the trailing edge, the nonrotated differencing scheme produced good results. Generally speaking, except for the expected reduction in convergence rate, no large freestream Mach number limitations (i.e., as $M_\infty \to 1$) have been observed.

C. Residual vs Error

Relative levels of convergence for AF2 and SLOR for given reductions in maximum residual are compared in Fig. 6. The solid line represents the final solution, which has been converged until the maximum residual dropped six orders of magnitude. The other results represent intermediate AF2 and SLOR solutions in which the maximum residual has been reduced by one, two, and three orders of magnitude. It is immediately obvious that reducing the maximum residual by equal amounts for AF2 and SLOR does not produce intermediate results with the same level of error. In fact, the error reduction for these two schemes can be substantially different for the same degree of residual reduction. For instance, the AF2 solution after a two-order-of-magnitude reduction in maximum residual (Fig. 6b) is closer to the final solution than is the SLOR solution after a residual drop of three orders of magnitude (Fig. 6c).

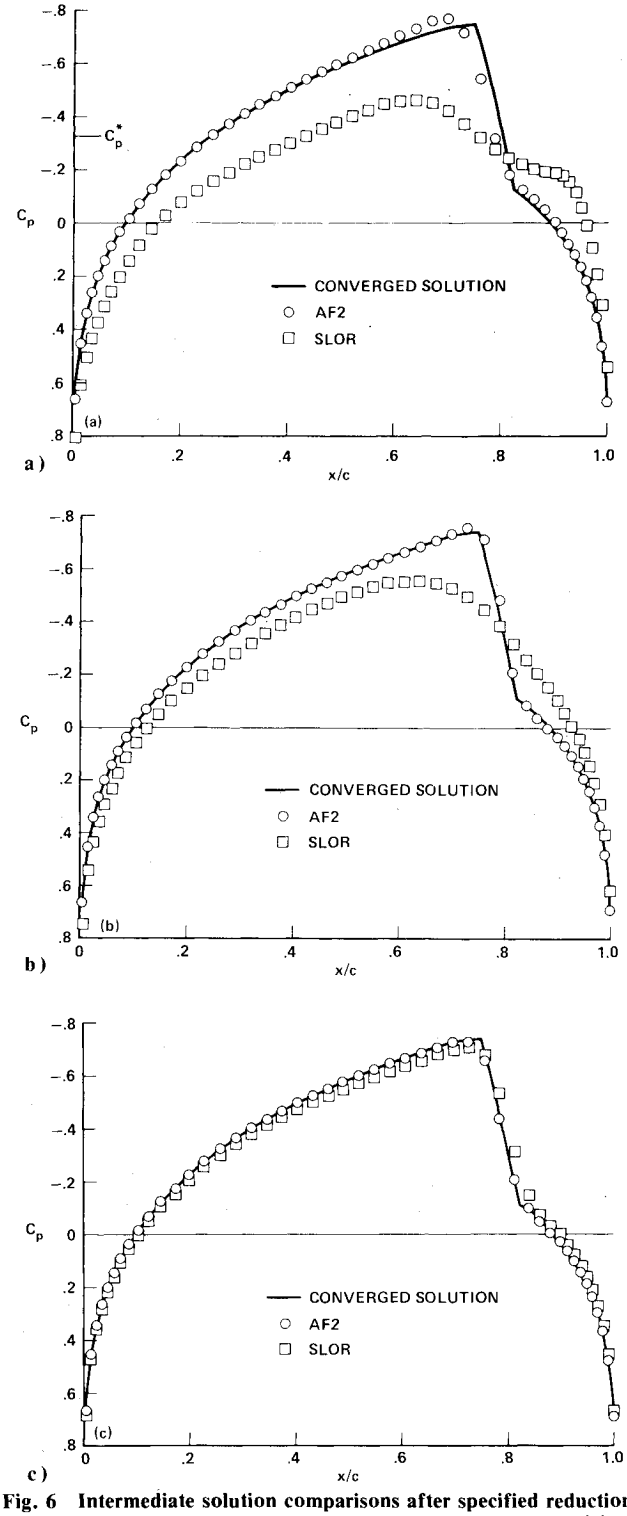

Fig. 6 Intermediate solution comparisons after specified reductions in the maximum residual (case B, optimum convergence). a) $|R|_{max}$ reduced one order of magnitude, b) $|R|_{max}$ reduced two orders of magnitude, c) $|R|_{max}$ reduced three orders of magnitude.

This behavior can also be observed by comparing the maximum residual history curves of Fig. 4 with the rms error history curves given in Fig. 7. The rms error at iteration n (E^n_{rms}) was computed from the surface pressure coefficient distribution by the following formula:

$$E^n_{\text{rms}} = \left[\frac{\sum_{i=i_{LE}}^{i_{TE}} \left(C^n_{p_i} - \bar{C}_{p_i}\right)^2}{i_{TE} - i_{LE} + 1} \right]^{\frac{1}{2}} \tag{29}$$

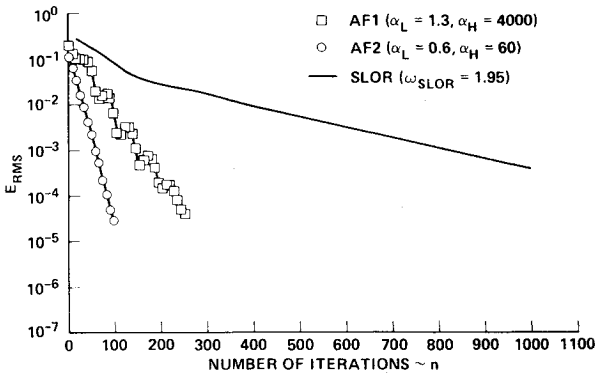

Fig. 7 rms error convergence history comparison (case B).

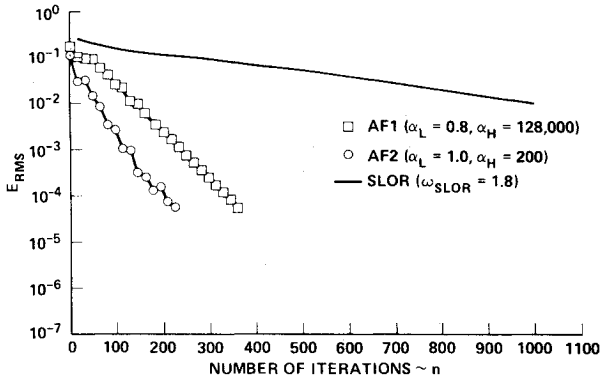

Fig. 8 rms error convergence history comparison (case B, nonoptimal convergence).

where $C_{p_i}^n$ is the surface pressure coefficient at the ith grid point and the nth iteration, $\bar{C}_{p_i}$ is the surface pressure coefficient at the ith grid point taken from the converged solution, and i_{LE} and i_{TE} are the indices indicating the leading- and trailing-edge grid points. The SLOR residual drops very rapidly initially and then levels off. The SLOR rms error drops gradually. Therefore, at the "knee" in the residual history curve, even though the residual has dropped by about three orders of magnitude, the actual rms error has dropped by only one order of magnitude. In contrast, both maximum residual and rms error results for the AF schemes are nearly straight lines with about the same slope.

This behavior is the result of two factors[2]: 1) the AF2 scheme treats all error components equally well (approximately), whereas the SLOR scheme performs efficiently on only the high-frequency error components; and 2) it can be shown that the residual is a weighted sum of errors, over the entire error frequency spectrum, weighted by the eigenvalue of the finite-difference scheme. The eigenvalue for the high-frequency error components is $O(\Delta x^{-2})$, and for the low-frequency error components is O(1). Hence, the residual is influenced heavily by the high-frequency errors. During the initial phase of a calculation, equal residual drops for AF2 and SLOR indicate the same drop in high-frequency error, but the reduction rates for the low-frequency errors are significantly different. For this reason, the AF approach reduces the total error much faster, and, consequently, the solution evolves much more rapidly. Therefore, the maximum residual operator should not be used as the basis for comparison between AF and SLOR schemes. Root-mean-square errors are much better suited for this purpose. In practice, use of the maximum residual operator for either AF or SLOR is the most convenient method for monitoring convergence (since the error is unknown). However, the convergence criterion must be adjusted in accordance with the solution procedure in use.

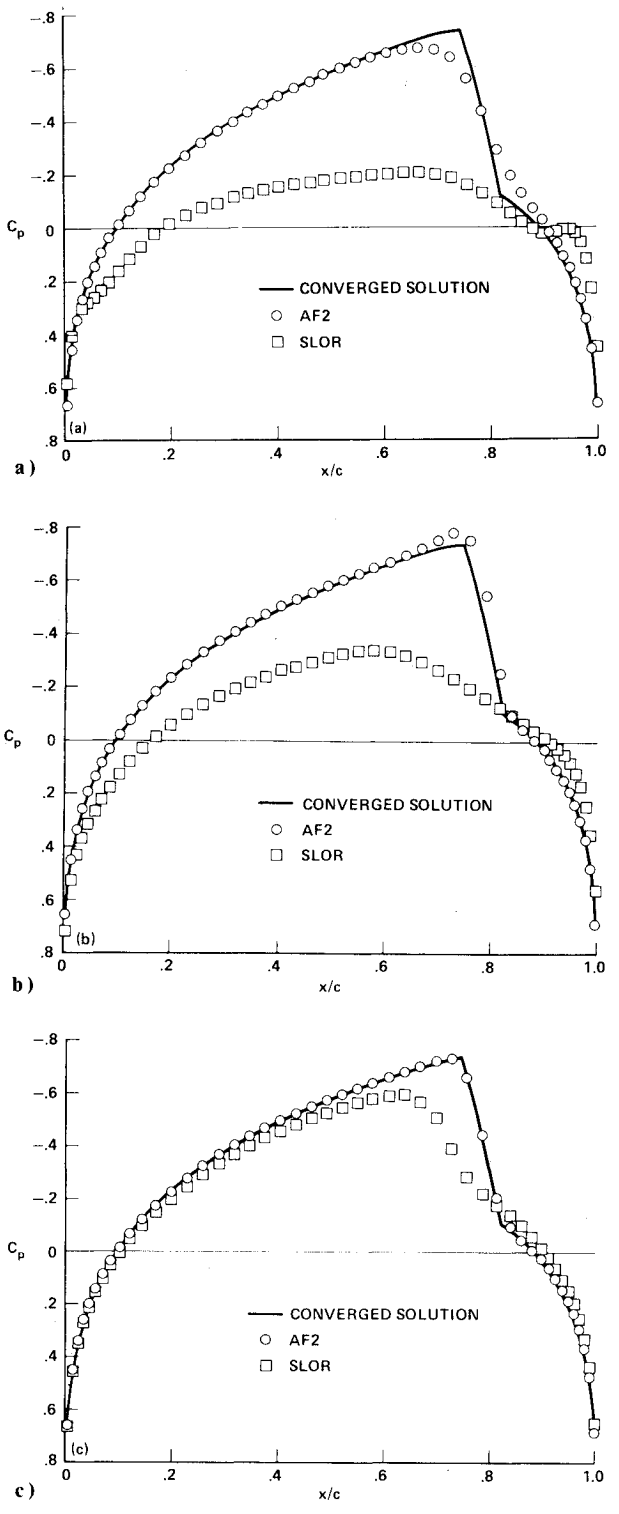

Fig. 9 Intermediate solution comparisons after specified reductions in the maximum residual (case B, nonoptimal convergence), a) $|R|_{max}$ reduced one order of magnitude, b) $|R|_{max}$ reduced two orders of magnitude, c) $|R|_{max}$ reduced three orders of magnitude.

D. Use of Nonoptimal Convergence Parameters

Only "optimal" convergence (i.e., cases with convergence parameters adjusted for optimal convergence) has been considered thus far. Because in practice the optimal values for α_H, α_L, and ω_{SLOR} are not known a priori, it is of interest to know the effect of nonoptimal parameters on the convergence speed. The rms error histories for AF1, AF2, and SLOR for nonoptimal parameters are shown in Fig. 8. The nonoptimal SLOR relaxation factor was chosen to be 1.8, and the α_H and α_L parameters for AF1 and AF2 were chosen from Eqs. (23)

and (24). For a four-order-of-magnitude reduction in rms error (which is well beyond plottable accuracy), nonoptimal AF2 is about 2.5 times slower than the optimal AF2 results. The AF1 and SLOR results are affected similarly, being about 1.5 and 3 times slower, respectively. For the nonoptimal case, in terms of iteration count, AF2 is about 1.5 times faster than AF1 and about 12 times faster than SLOR.

Another indication of how fast the AF2 scheme can establish the global solution even for nonoptimal acceleration parameters is shown in Fig. 9. The solid line in each case is the final solution, which has been converged until the maximum residual dropped six orders of magnitude. The other results presented are AF2 and SLOR intermediate solutions in which the maximum residual has been reduced by one, two, and three orders of magnitude. As before (Fig. 6), it again is obvious that reducing the maximum residual by equal amounts for AF2 and SLOR solutions does not produce equivalent error reduction. In the present nonoptimal case, the difference between the AF2 and SLOR solutions for a given drop in residual is even larger than in the previous optimum case. This is because the smaller value of ω_{SLOR} used in the nonoptimum case puts even more emphasis on the high-frequency errors, thus causing the SLOR residual to drop faster, whereas the rms error is dropping slower.

V. Conclusions

New, fully implicit algorithms for solving the full potential equation in conservation form have been developed. These new schemes are of the approximate factorization variety. Computed results indicate a substantial increase in computational efficiency over an SLOR algorithm.

The spatial difference scheme used to approximate the full potential equation is equivalent to the one developed by Jameson. However, in the present approach, the artificial viscosity required to maintain stability in supersonic regions is not added explicitly. It is introduced by spatially retarding the density in the finite-difference equation. This strategy greatly simplifies the solution procedure, so that only bidiagonal or tridiagonal matrix operations are required.

Results indicate that the standard measure of convergence (i.e., a specified reduction in the maximum residual) is not a good means for comparing AF and SLOR convergence rates. Using the maximum residual as a criterion to determine relative levels of convergence for either technique individually is not questioned. However, AF schemes definitely reach a greater degree of convergence in terms of the error at higher residuals than do SLOR techniques.

The new AF schemes, although applied in this paper only to circular-arc airfoils with small-disturbance boundary conditions and Cartesian finite-difference grids, are extendible to arbitrary geometries in both two- and three-dimensional flows. The principal difficulty is the handling of the cross-derivative terms arising from general geometry transformations. Solutions for cases with airfoil-adapted grids have been obtained, and the efficiency of the AF procedure does carry over to these more practical flows.[9]

Acknowledgment

The authors express their gratitude to Joseph L. Steger for his many helpful suggestions during the course of this study.

References

[1]Ballhaus, W.F., Jameson, A., and Albert, J., "Implicit Approximate Factorization Schemes for the Efficient Solution of Steady Transonic Flow Problems," *AIAA Journal*, Vol. 16, June 1978, pp. 573-579.

[2]Ballhaus W.F., "A Fast Implicit Solution Procedure for Transonic Flows," *Third International Symposium on Computing Methods in Applied Sciences and Engineering*, Versailles, France, Dec. 5-9, 1977.

[3]Jameson, A., "Transonic Potential Flow Calculations Using Conservative Form," *AIAA Second Computational Fluid Dynamics Conference Proceedings*, June 1975, pp. 148-155.

[4]Steger, J.L. and Baldwin, B.S., "Shock Waves and Drag in the Numerical Calculation of Isentropic Transonic Flow," NASA TN D-6997, 1972.

[5]Lax, P.D., "Weak Solutions of Nonlinear Hyperbolic Equations and Their Numerical Computation," *Communications on Pure and Applied Mathematics*, Vol. 7, No. 1, 1954, pp. 159-193.

[6]Murman, E.M., "Analysis of Embedded Shock Waves Calculated by Relaxation Methods," *Proceedings of AIAA Computational Fluid Dynamics Conference*, Palm Springs, Calif., July 1973.

[7]Jameson, A., "Transonic Flow Calculations," *Computational Fluid Dynamics,* VKI Lecture Series, von Karman Inst. for Fluid Dynamics, Rhode-St-Genese, Belgium, March 15-19, 1976.

[8]Ballhaus, W.F. and Steger, J.L., "Implicit Approximate Factorization Schemes for the Low-Frequency Transonic Equations," NASA TM X-73,082, 1975.

[9]Holst, T.L., "An Algorithm for the Conservative Transonic Full Potential Equation Using an Arbitrary Mesh," AIAA Paper 78-1113, July 1978.

[10]Jameson, A., private communication, Jan. 1978.